Journal of Inorganic Biochemistry 201 (2019) 110810

Contents lists available at ScienceDirect

Journal of Inorganic Biochemistry

journal homepage: www.elsevier.com/locate/jinorgbio

High antiparasitic activity of silver complexes of 5,7-dimethyl-1,2,4-triazolo [1,5 *a*]pyrimidine

Ginés M. Esteban-Parra[a,*], José M. Méndez-Arriaga[a], Antonio Rodríguez-Diéguez[a], Miguel Quirós[a], Juan M. Salas[a,1], Manuel Sánchez-Moreno[b]

[a] Department of Inorganic Chemistry, University of Granada, Avda. Severo Ochoa s/n, 18071 Granada, Spain
[b] Department of Parasitology, University of Granada, Avda. Severo Ochoa s/n, 18071 Granada, Spain

ARTICLE INFO

Keywords:
Triazolopyrimidines
Metal complexes
Silver
Antiparasitic activity
Leishmaniasis
Chagas disease

ABSTRACT

Two dinuclear silver complexes containing 5,7-dimethyl[1,2,4]triazolo[1,5-*a*]pyrimidine (dmtp) were synthesized, $[Ag_2(dmtp)_3]_2[Ag_2(dmtp)_2](BF_4)_6(H_2O)_2$ and $[Ag_2(dmtp)_2(ClO4)_2][Ag_2(dmtp)_2(H_2O)_2](ClO_4)_2$. They have been spectroscopically and thermally characterized and their structures have been solved by single crystal X-ray diffraction. The compounds display fluorescence in the visible range (486 nm) when irradiated with UV light (265 nm). Both compounds, together with a previously reported analogue containing nitrate as counteranion, were assayed *in vitro* against three different species of *Leishmania* spp. and *Trypanosoma cruzi*, (parasites responsible for Leishmaniasis and Chagas disease) showing an extremely high antiparasitic activity, with IC_{50} values below the lower tested concentration (1 μM) for the three compounds and the four microorganisms, and hence a selectivity index better than those of the reference commercial drugs by more than one magnitude order, also improving the results of the free ligand and previously reported complexes with metals of the first transition series.

1. Introduction

Triazolopyrimidine derivatives and, more specifically, those belonging to the 1,2,4-triazolo[1,5-*a*]pyrimidine (tp) family, have been widely used as ligands in coordination chemistry, due to their ability to coordinate metal ions through different nitrogen atoms [1–3]. Scheme 1 displays the 5,7-dimethyl derivative (used in this work) indicating the IUPAC numbering scheme used for these heterocycles.

For more than two decades, the coordination chemistry of heterocycles of the tp family has been studied by our research group [4–13], as well as by others [14–20]. The involved tp derivatives usually differ in the residues attached to positions 5 and 7: methyl, phenyl, amino, hydroxyl (in the latter case the keto tautomer is usually present), *etc.* These derivatives are considered as mimetic of purine bases of DNA, changing the nitrogen that would be present at position 6 by the bridgehead nitrogen at position 8, which is not accessible for metal binding. This mimesis makes these compounds suitable for biological applications, like anticancer [21,22] or bactericidal [23,24].

In the past few years, our interest has been mainly focused on antiparasitic activity, specifically against *Leishmania* spp. and *Trypanosoma cruzi*, pathogenic agents of Leishmaniasis and Chagas disease, respectively. Both are considered as neglected diseases and affect mainly to tropical and subtropical regions, with Leishmaniasis being endemic in almost 100 countries and Chagas disease currently affecting to 8–10 million people [25–27]. The existing treatments for these illnesses are based in pentavalentantimonials (Glucantime, Pentostam) in the case of Leishmaniasis, and nitro heterocyclic derivatives (Nifurtimox, Benznidazole) for the Chagas disease treatment. However, those drugs were developed more than five decades ago, and they present serious side effects and can cause resistance for the pathogens. Due to this, there is an urgent need of developing new and more specific drugs.

The antiparasitic activity of many compounds has been studied by different research groups in the last years, highlighting a synergistic effect when a metallic centre is coordinated to bioactive organic ligands [28–30]. With this aim, our group has designed several complexes that have shown interesting antiparasitic activities, involving different triazolopyrimidine derivatives and metal ions mostly belonging to the first transition series [31–35], although Ru [36] and f-block elements [37] have also been tested. In these studies, we have found several examples of compounds with antiprotozoal activity similar or somewhat better than the actually used drugs but appreciably less toxic to

* Corresponding author.
E-mail address: gmesteban@ugr.es (G.M. Esteban-Parra).
[1] Professor Juan Manuel Salas passed away on November 5, 2018.

https://doi.org/10.1016/j.jinorgbio.2019.110810
Received 2 May 2019; Received in revised form 22 August 2019; Accepted 24 August 2019
Available online 29 August 2019
0162-0134/

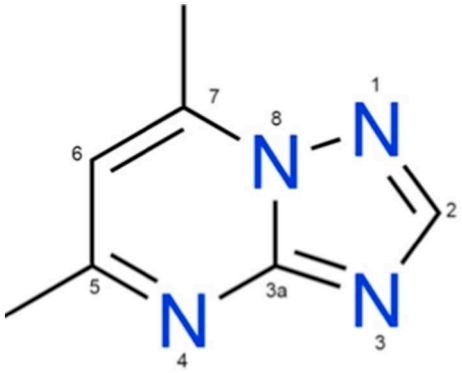

Scheme 1. Structure of 5,7-dimethyl-1,2,4-triazolo[1,5-a]pyrimidine (dmtp).

somatic cells, thus yielding selectivity indexes substantially better than these reference drugs.

Following these results, we have decided to try silver due to its well-known antimicrobial activity. We have synthesized and characterized two new silver-based complexes containing 5,7-dimethyl[1,2,4]triazolo [1,5-*a*]pyrimidine (**dmtp**) as ligand and perchlorate and tetrafluoroborate as counteranions, the molecular formula of which are $[Ag_2(dmtp)_3]_2[Ag_2(dmtp)_2](BF_4)_6(H_2O)_2$ and $[Ag_2(dmtp)_2(ClO4)_2]$ $[Ag_2(dmtp)_2(H_2O)_2](ClO_4)_2$. In addition, *in vitro* antiparasitic activity of both compounds and another analogous one previously characterized ($[Ag_2(dmtp)_2(NO_3)_2]$) [38] was assayed against extracellular forms of three species of *Leishmania spp*. (*L. infantum*, *L. donovani* and *L. braziliensis*) and against *T. cruzi*, as well as their cytotoxicity in host cells (macrophage J774.2 and Vero cells). The results have been compared with values found for reference drugs and free dmtp, finding that the activity of the silver compounds clearly improve, not only that of reference drugs, but also that displayed by complexes of other metal cations.

2. Experimental

2.1. Materials and methods

All metallic salts and **dmtp** ligand used as reagents were purchased from commercial sources and used as received without further purification.

2.2. Preparation of $[Ag_2(dmtp)_3]_2[Ag_2(dmtp)_2](BF_4)_6(H_2O)_2$ (1)

A solution of 2 mmol (0.296 g) of **dmtp** in 10 mL of water was added to an aqueous solution (10 mL) of $AgBF_4$ (2 mmol, 0.389 g). The resulting solution was left at room temperature in the dark. After 48 h, colourless prismatic crystals suitable for XRD measurements appeared and were collected by vacuum filtration.

Anal. Calcd. for $C_{56}H_{68}N_{32}O_2B_6F_{24}Ag_6$ C, 28.15; H, 2.87; N, 18.76. Found: C, 28.32; H, 2.96; N, 18.69%. FT-IR: Yield: ~ 65%.

2.3. Preparation of $[Ag_2(dmtp)_2(ClO4)_2][Ag_2(dmtp)_2(H_2O)_2](ClO_4)_2$ (2)

A solution of 2 mmol (0.296 g) of dmtp in 10 mL of $HClO_4$ 1 M was added to a solution (10 mL) of $AgClO_4$ (2 mmol, 0.415 g) in the same solvent. After 24 h at room temperature in the dark, colourless prismatic crystals suitable for XRD measurements appeared and were collected by vacuum filtration.

Anal. Calcd. for $C_{28}H_{36}N_{16}O_{18}Cl_4Ag_4$ C, 23.07; H, 2.49; N, 15.37. Found: C, 22.94; H, 2.56; N, 15.54%. FT-IR: Yield: ~83%.

2.4. Preparation of $[Ag_2(dmtp)_2(NO_3)_2]$ (3)

Compound **3** was prepared as a variation of the previously described procedure [38]. A solution of 2 mmol (0.296 g) of dmtp in 10 mL of HNO_3 was added to solution of $AgNO_3$ (2 mmol, 0.321 g) in the same solvent. The solution was left at room temperature in darkness during 72 h. Finally, colourless prismatic crystals appeared and were collected by vacuum filtration.

Anal. Calcd. for $C_{14}H_{16}N_{10}O_6Ag_2$ C, 26.44; H, 2.54; N, 22.02. Found: C, 26.32; H, 2.62; N, 22.09%. FT-IR: Yield: ~85%.

2.5. Physical measurements

Elemental analyses were carried out at the "Centro de Instrumentación Científica" of the University of Granada on a THERMO SCIENTIFIC analyser model Flash 2000. The IR spectra of powdered samples were recorded with a BRUKER TENSOR 27 FT-IR and OPUS data collection program. Solid-state photoluminescence spectra were recorded at room temperature with a Varian Cary-Eclipse Fluorescence Spectrofluorimeter. Thermal behaviour (thermogravimetry – TG – and differential scanning calorimetry – DSC) was studied under an air flow in Shimadzu TGA-50 and Shimadzu DSC-50 equipments at heating rates of 20 and 10 °C min^{-1}, respectively. NMR spectra were collected with a high definition 500 MHz NMR spectrometer BRUKER Avance NEO using D_2O as solvent.

2.6. Single-crystal structure determination

Crystals of complexes **1** and **2** were mounted on a glass fibre and used for data collection on a Bruker Smart diffractometer equipped with an APEX detector and graphite monochromated CuKα (**1**) or *MoKα* (**2**) radiation (λ = 1.54178 and 0.71073 Å, respectively). The data reduction was performed with the APEX2 [39] software and the absorption correction with SADABS [40]. The structures were solved by direct methods and anisotropically refined by full-matrix least-squares on F^2 by means of the SHELX-14 program package [41]. Two of the tetrafluoroborate anions in **1** and one of the perchlorate anions in **2** were found to be disordered between two positions. Powder X-ray diffraction patterns of compounds **1** and **2** (supplementary material: Figs. S1–S2) confirm the crystalline homogeneity of the samples. Powder DRX data were collected on a Bruker D2 Phaser diffractometer with monochromated CuKα radiation (λ = 1.5405 Å) over the range $5 < 2\theta < 35°$.

2.7. Parasite strain and culture

Promastigote forms of *L. infantum* (MCAN/ES/2001/UCM-10), *L. braziliensis* (MHOM/BR/1975/M2904), *L. donovani* (LCRL133LRC) and epimastigote forms of *Trypanosoma cruzi* (IRHOD/CO/2008/SN3) were cultivated *in vitro* in medium trypanosome liquid (MTL) [Hank's Balanced Salt Solution (HBSS) (Gibco), $NaHCO_3$, lactalbumin, yeast extract, bovine haemoglobin and antibiotics] with 10% inactive fetal bovine serum and were kept in an air atmosphere at 28 °C, in Roux flasks (Corning, USA) with a surface area of 75 cm^2, according to the methodology described by Gonzalez et al. [42]. The screening of extracellular forms of parasites was carried out using 24-well plates with MTL medium and 5×10^4 parasites per well. The products were tested at 1, 10, 25 and 50 μM, prepared from mother aqueous solutions of the compounds, leaving some wells without drugs as control, and were incubated at 28 °C during 72 h before the parasite final count.

2.8. Cell culture and cytotoxicity test

The cytotoxicity tests for macrophages and Vero cells were performed at the Cell Experiment Unit in the "Centro de Instrumentación Científica" of the University of Granada, according to the methodology

described below. The experiment was carried out in 96-well plates to be measured in the ELISA reader. The growth inhibition of mammalian cells was studied using macrophages for the three strains of *Leishmania* spp. and Vero cells for *T. cruzi*. J774.2 macrophages (European Collection of Cell Culture – ECACC – number 91051511), which were originally obtained from a tumour in a female BALB/c rat in 1968, were grown in a minimum essential medium (MEM) plus glutamine (2 mM) and supplemented with 20% inactivated fetal bovine serum (FBS). Vero cells (Flow) were grown in Roswell Park Memorial Institute medium (RPMI), which was supplemented with 10% inactivated fetal bovine serum. Both cell cultures were incubated in a humidified 95% air, 5% CO_2 atmosphere at 37 °C for several days. The products were tested at 50, 100, 200 and 400 μM. First, the cells were sowed in a 96-well plate (2500 cells/well for macrophages and 3500 cells/well for Vero cells) to a volume of 100 μL/well and then were incubated at 37 °C with 5% CO_2 during 24 h. The complexes solutions were prepared in advance corresponding to the average growing cells (RPMI 10% FBS for Vero cells and MEM + Glut 20% FBS for macrophages) at the double of the highest concentration to be tested. The solutions were performed in a sterile bath with the different channels, by adding 100 μL of complex solution or medium (only adding medium in the control wells) to the corresponding well. After that, the plate was incubated at 37 °C with 5% CO_2 for 48 h. Two days after, 20 μL of Alamar Blue dye (10% of the volume of the well) were added to each well and incubated at 37 °C with 5% CO_2 during another day. The whole incubation time once the products were added was 72 h, coinciding with the screening period to have comparable selectivity index (SI) results. Finally, the plate was read with an ELISA reader with Alamar Blue.

2.9. Studies on the mechanism of action

For the studies of mechanism of action, extracellular forms of the parasites of *L. infantum* and *L. braziliensis* were incubated in a final volume of 3 mL of MTL medium, in a final concentration of 5×10^6 parasites/mL, for 72 h with a 0,5 μM concentration of drug; additionally, a control of both strains was prepared in the same conditions without adding the compound. Once passed the incubation time, the samples were centrifugated at 2500 rpm for 10 min. After that, the supernatant liquid was collected to its further analysis by ^{1}H NMR to determine excreted metabolites as previously described by Fernandez-Becerra et al. [43]. The chemical displacements used to identify the respective metabolites were consistent with those described by Fernandez-Becerra et al. [43]

3. Results and discussion

3.1. Crystal structure of $[Ag_2(dmtp)_3]_2[Ag_2(dmtp)_2](BF_4)_6(H_2O)_2$ (1)

Compound **1** crystallizes in the monoclinic space group *P21/c*. Details of the structure determination and the refinement of the complex are summarized in Table 1. A list of bond lengths and angles is given in the supplementary material (Table S1). Two different kinds of dinuclear entities appear in the crystal structure of **1**: the first one involving two dmtp moieties (type A) and the other including three of them (type B). "Type A" entities are placed in crystallographic inversion centres whereas "type B" ones are placed in general position, hence two "type B" complexes are present for each "type A". A view of both dinuclear units is shown in Fig. 1. Type A dimers are planar, with each silver atom linearly coordinated to the N3 atom of one dmtp molecule (Ag—N3 distance, 2.287(7) Å) and to the N4 of the other (Ag—N4 distance, 2.297(6) Å) closing an eight-membered $Ag_2C_2N_4$ ring, this kind of ring having been frequently found in silver complexes of triazolopyrimidine derivatives [44]. Ag—Ag distance within the dimer is 2.941(1) Å, possibly too long to be considered as an Ag—Ag bond but short enough to be regarded as an argentophilic interaction, which is supported by previously reported theoretical calculations [38]. On the other hand, silver atoms in the "type B" dinuclear complex have a distorted trigonal planar environment defined by one N-atom of each of the three present dmtp ligands. Both Ag atoms are not equivalent, one of them is linked to one N3 and two N4 atoms whereas, reciprocally, the other one is linked to one N4 and two N3 atoms. This kind of dinuclear complex is much less frequent than the "type A", only one previous example having being reported with unsubstituted 1,2,4-triazolo-[1,5-a]-pyrimidine [45]. The trigonal geometry is severely distorted, with Ag—N distances comprised in a wide range (2.14–2.38 Å) and N-Ag-N angles considerably departing from 120°. The silver-silver distance is

Table 1
Crystallographic data and structural refinement details for **1** and **2.**

Compound	1	2
Chemical formula	$C_{56}H_{68}N_{32}O_2B_6F_{24}Ag_6$	$C_{28}H_{36}N_{16}O_{18}Cl_4Ag_4$
CCDC	1893468	1893467
COD	3000218	3000219
M/g mol^{-1}	2389.39	1457.97
T/K	100(2)	100(2)
Cryst. syst.	Monoclinic	Triclinic
Space group	P 2_1/c	P-1
a (Å)	12.0038(3)	8.9978(4)
b(Å)	27.5554(8)	10.8619(5)
c(Å)	12.8479(4)	12.0576(6)
α (°)	90	100.5189(16)
β (°)	100.9670(10)	105.2550(16)
γ (°)	90	93.1937(17)
V/ Å^3	4172.1(2)	1111.09(9)
Z	2	2
ρ/g cm^{-3}	1.619	2.179
μ/mm^{-1}	1.902	2.069
GOF[a]	1.044	1.059
R_{int}	0.0615	0.0326

[a] $S = [\Sigma w(F_0^2 - F_c^2)^2 / (N_{obs} - N_{param})]^{1/2}$.

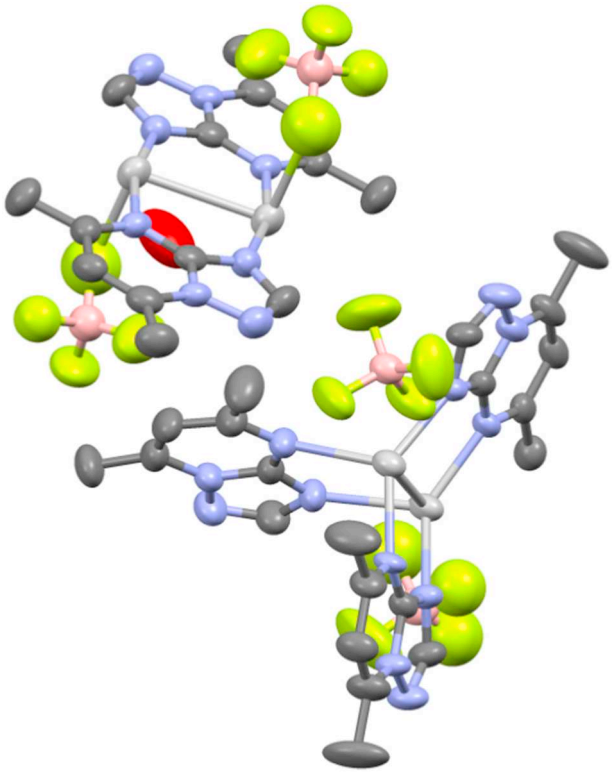

Fig. 1. Crystal structure of $[Ag_2(dmtp)_3]_2[Ag_2(dmtp)_2](BF_4)_6(H_2O)_2$**(1)** Colour code: silver, light grey; nitrogen, blue; carbon, grey; oxygen, red; boron, pink; fluorine, yellow-green. (For interpretation of the references to colour in this figure legend, the reader is referred to the web version of this article.)

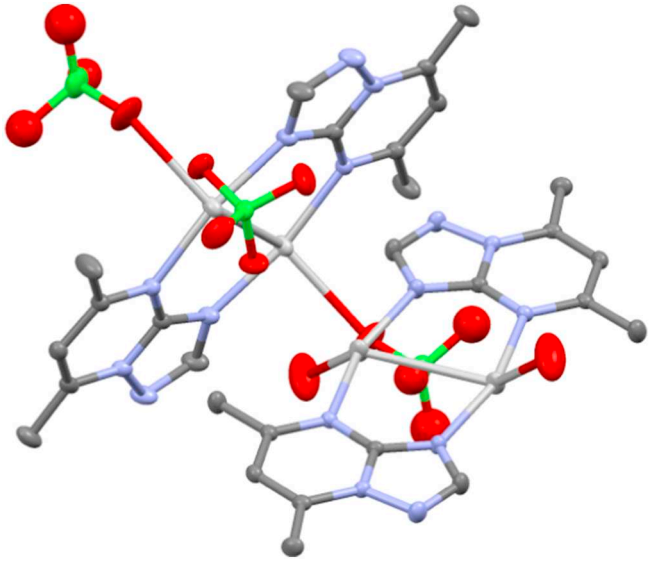

Fig. 2. Crystal structure of $[Ag_2(dmtp)_2(ClO4)_2][Ag_2(dmtp)_2(H_2O)_2](ClO_4)_2$**(2)**. Colour code: silver, light grey; nitrogen, blue; carbon, grey; oxygen, red; chlorine, green. (For interpretation of the references to colour in this figure legend, the reader is referred to the web version of this article.)

3.0580(8) Å, appreciably longer than in the "type A" dimer. The charge of those cationic dinuclear complexes is balanced by tetrafluoroborate ions, three of them per asymmetric unit, two of which being disordered between two alternative positions. One of the disordered components of one of the anions weakly interacts with the silver atom in the "type A" dimer (Ag—F distance, 2.489(15) Å) perpendicularly to the ring plane. The asymmetric unit is completed by one interstitial water molecule, the whole packing of the structure being supported by weak Van der Waals forces and weak H-bonds between the water molecule and the anions.

3.2. Crystal structure of $[Ag_2(dmtp)_2(ClO4)_2][Ag_2(dmtp)_2(H_2O)_2](ClO_4)_2$ (2)

Compound **2** crystallizes in triclinic *P-1* space group. Its crystal structure is shown in Fig. 2 and the details of the structure determination and refinement are compiled in Table 1. Selected bonds and angles are given in the supplementary material (Table S2). Like in the previous compound, the crystal structure also includes two crystallographically different dinuclear silver entities, but in this case both are placed in crystallographic inversion centres and feature a $Ag_2C_2N_4$ core, thus being analogous to the "type A" dimer present in compound **1**. The Ag—N3, Ag—N4 and Ag—Ag distances are 2.153(2), 2.173(2) and 2.9977(4) Å for the first of these dimers and 2.158(2), 2.187(2) and 3.0653(5) for the second. The main difference between both dimers is the presence of a moiety weakly coordinated to each silver atom, a perchlorate anion for the first dimer and a water molecule for the second. The corresponding Ag—O distances are 2.706(3) and 2.605(4) Å, respectively. The Ag—O bond is neither coplanar with the $Ag_2C_2N_4$ core nor perpendicular to it, but in an intermediate position as indicated by the O-Ag-Ag angles which are 130.4(1) and 127.4(1)° respectively. The coordinated perchlorate anion is disordered between two positions rotated to each other around the Cl-(coordinated O) bond. A crystallographically independent interstitial perchlorate anion is present balancing the charge. All present species are packaged to form the crystal interacting only by weak Van der Waals forces and weak H-bonds from the water molecules to perchlorate oxygen atoms.

3.3. Infrared spectra

Two characteristic bands in the 1700–1500 cm^{-1} region are present in the infrared spectrum of the **dmtp** ligand. One of them comes from the vibration mode of the triazolopyrimidinic skeleton (1638 cm^{-1}), while the second one corresponds to the pyrimidinic ring vibration (1548 cm^{-1}). Both are slightly affected by the metal coordination, with a small shift to higher frequencies. The spectra of the three complexes are very similar, as expected since the binding mode of the ligand is the same. The υ(O—H) vibration of water appears as two well-defined bands at 3560 and 3621 cm^{-1} (**1**) and at 3520 and 3598 cm^{-1} (**2**). The presence of coordinated BF_4^- and ClO_4^- anions in **1** and **2** respectively is indicated by a strong broad band around 1100 cm^{-1}, whereas the NO_3^- anion in **3** appears near to 1400 cm^{-1}. FT-IR spectra of these complexes have been collected as supplementary material (Figs. S3–S4).

3.4. NMR spectra

^{1}H NMR spectra (Figs. S7–S18) have been recorded for free dmtp and its silver complexes using D_2O as solvent to check the stability of the compounds in aqueous media. The free ligand presents the expected four signals at 2.54, 2.65 (CH_3), 7.01 (C6-H) and 8.38 (C2-H) ppm. The spectra of the tree complexes are almost identical with the methyl signals overlapped at 2.83 ppm., C6-H at 7.37 ppm. and C2-H at 8.63 ppm.

The presence of a single set of signals for the complexes, even for compound **1**, indicates that a fast interchange takes places in solution between different species probably also involving the free ligand and we can see in the spectra just the average value of the corresponding signals. Nevertheless, the differences between the signal positions in the free ligand and those in the complexes are large enough to ensure that a significant proportion of the ligand remains coordinated to the metal in the observed equilibrium. C2-H and C6-H signals display similar changes with respect to the free ligand, suggesting that both rings of the heterocycle are similarly involved in metal coordination and that the N3–N4 bridging is perhaps the main coordination mode also in solution.

The spectra do not change at all for the 72 h. following the preparation of the solutions. This indicates that the equilibrium is reached almost immediately and then remains unaltered.

3.5. Thermal behaviour

Thermal decomposition of compounds **1** and **2** starts with their dehydration process that takes place in one step that appears as broad weight losses (TG) and endothermic (DSC) effects centred at 96 (**1**) and 120 °C (**2**). The experimental weight losses are respectively 1.52 and 2.57%, matching the theoretical values (1.51 and 2.47%). Pyrolytic decomposition starts at 267 °C for **1** and at 305 °C for **2**, with a strong exothermic peak in the DSC diagrams and a sudden weight loss at the TG. Then it continues more slowly until the end of the experiment at 920 °C, the TG curve not being horizontal at the end, this possibly meaning the presence of slowly burning carbonaceous material. This may explain why the residue in **1** (32.8%) is higher than expected for metallic silver (25.3%), that should be the residue if the organic part were completely pyrolized. For **2**, the explosive decomposition of perchlorate provokes the projection of material outside the crucible, with a very low residue remaining at the final temperature. TG and DSC diagrams are included in the supplementary material (Figs. S5–S6).

3.6. Fluorescent emission

Due to their extended aromaticity and the presence of polyheterosubstituted rings, triazolopyrimidinic heterocycles are good candidates to show photoluminescent properties [46], especially when they are coordinated to metallic ions. In fact, 7-amino[1,2,4]triazolo

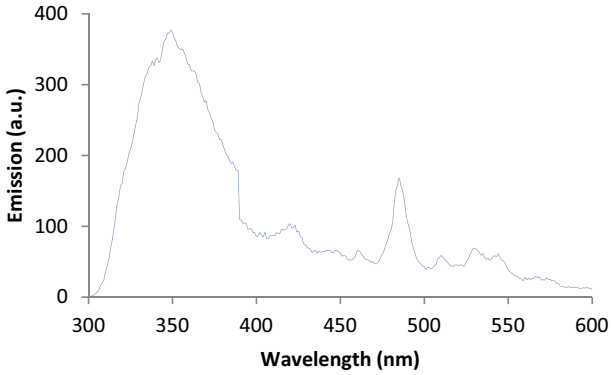

Fig. 3. Emission spectrum of dmtp when excited at 265 nm.

[1,5-*a*]pyrimidine (7-atp) and 7-hydroxy-5-methyl[1,2,4]triazolo[1,5-*a*]pyrimidine (HmtpO) have shown an increase in their intrinsic fluorescent emission when coordinated to zinc or cadmium [12,47,48]. However, there are no previously reported studies on luminescent emission for dmtp or any of its metal complexes. The UV absorption spectrum of dmtp has a maximum at 265 nm, hence the fluorescent spectrum of dmtp (Fig. 3) has been recorded exciting with UV light of this wavelength. This emission spectrum shows three maxima: the most intense one is centred at 350 nm, a second one of medium intensity appears at 485 nm and a third one, barely observed, is centred at 420 nm.

When solid samples of compounds **1** and **2** are exposed to UV light at room temperature, they show light-blue fluorescent emission. When excited with UV light of 265 nm., both compounds display a very similar emission spectrum (Fig. 4), with three bands at 365, 420 and 486 nm., these wavelengths being similar to those displayed by the free ligand but with important changes in the relative intensity, the two bands in the visible region becoming much more intense. Analysing these two bands, it was found that the characteristic excitation wavelength is the same for both bands but it is not the same for both compounds, the corresponding values being 236 and 254 nm, for **1** and **2** respectively. The emission spectra of the compounds when excited with UV of these wavelengths (Fig. 5) feature a further increase in the intensity of the bands in the visible region, more noticeably that at 486 nm whereas that at 365 nm virtually disappears. These results show how the coordination to silver modulates the fluorescent emission of dmtp, making the main peak in the UV region almost disappear whereas the secondary ones in the visible region become much more intense. From a practical point of view, the emission moves from UV to visible range.

3.7. In vitro antiparasitic activity and cytotoxicity

Taking into account the synergistic influence of metal coordination on the biological activity of triazolopyrimidine ligands, we decided to analyse the leishmanicidal and trypanosomicidal efficacy of complexes **1–3**. As explained in the experimental section, antiproliferative experiment against extracellular promastigote (*Leishmania* spp.) or epimastigote (*Trypanosoma cruzi*) forms of the parasites were carried out. After this, a cytotoxicity assay was performed in order to check whether a good antiparasitic behaviour fighting extracellular forms of infective agents produces also damage in the host cells. The quotient between the host cells cytotoxicity and extracellular antiproliferative efficacy (selectivity index or SI) gives us an idea of the suitability of the compounds as prodrugs.

The antiproliferative assays for the three complexes (**1–3**) indicated a great activity in all cases, since the lower tested concentration in our protocol (1 μM) of any of the three complexes was enough to produce an inhibition higher than 50% in the growing of any of the four parasites (Fig. S19), this meaning that the corresponding IC_{50} values are all of them below 1 μM. Table 2 display these results, comparing with the values obtained for free dmtp, for the reference drugs currently used in the treatment of the parasites and for a few selected metal complexes of triazolopyrimidine derivatives previously reported by our research group. The antiproliferative properties of the silver complexes clearly improve the results of all other dmtp and mtpO complexes in the Table 2 and are as good as those of the nickel complexes of 4,6-dimethyl-1,2,3-triazolo-[4,5-d]-pyrimidin-5,7-dione (Hdmax) [50].

On the other hand, cytotoxicity experiments were also positive, being in a similar range than the free ligand for **1** and **3** against macrophages, but with a remarkable value for **2**, which is non-toxic for macrophages even at the highest tested concentration. For Vero cells, the cytotoxicity values were more than twice better than those of the free ligand for **2** and **3**, while for complex **1** was virtually the same. With these results, we can establish lower limits for the SI values that are more than one order of magnitude higher than the SI values of dmtp, about two orders of magnitude higher than the reference drugs or even three for the most outstanding cases, that are those of **2** against the three *Leishmania* spp. strains, making it an excellent candidate for further studies both *in vitro* and *in vivo*. Comparing with previous results of metal complexes of this kind of heterocycles, we see that the three silver complexes display better SI values for *T. cruzi*. And regarding the *Leishmania* parasites, complexes **1** and **3** are in the same range than a Cu-dmtp [32] and a few lanthanide-mtpO [37] compounds, whereas **2** has a much better behaviour. A more complete comparison may be performed using the updated review published by Salas et al. [3].

In order to check whether the metal ion by itself might be the responsible for the observed antiparasitic activity, assays were performed with the silver salts (tetrafluoroborate, perchlorate and nitrate), the results being also collected at Table 2. We can see that these salts present IC_{50} values comparable to the reference drugs and much higher than compounds **1**, **2** and **3**. On the other hand, the cytotoxicity data indicate that the metal salts are extremely toxic for the host cells even at the lowest tested concentration (50 μM) resulting in selectivity

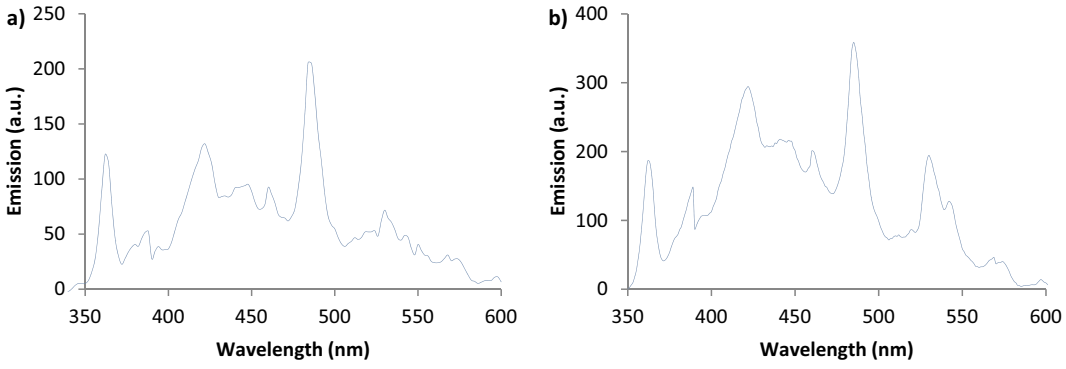

Fig. 4. Emission spectra of compound **1** (a) and compound **2** (b) excited at 265 nm.

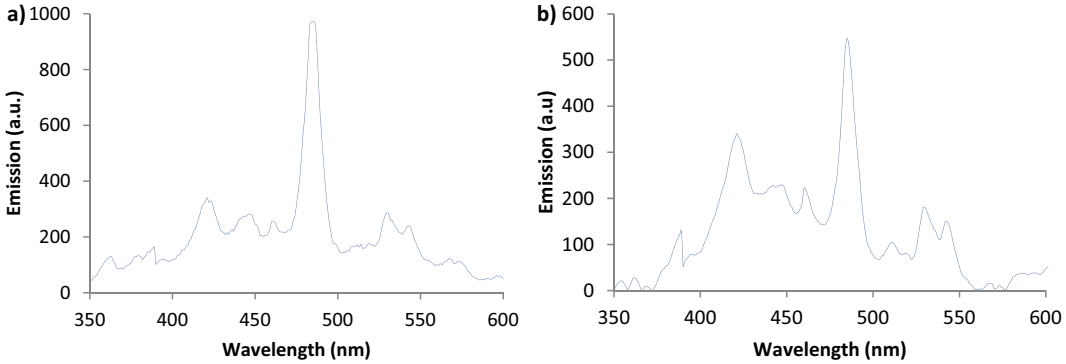

Fig. 5. Emission spectra of compound **1** (a) excited at 236 nm and compound **2** (b) excited at 254 nm.

Table 2
In vitro activity of **dmtp**, complexes 1–3 and reference drugs against promastigote forms of *Leishmania* spp., epimastigote forms of *Trypanosoma cruzi*, J774.2 macrophages and Vero cells after 72 h of incubation at 37 °C. Previous results of other tp derivatives complexes are included for comparison.

Compound	IC_{50} ± SD(μM)[a] and selectivity index[b] (SI)						
	L. infantum	*L. braziliensis*	*L. donovani*	*T. cruzi*	J774.2 macro.	Vero cells	Ref.
Glucantime	18.0 ± 0.6 **SI:** 0.8	25.6 ± 1.6 **SI:** 0.6	26.6 ± 5.4 **SI:** 0.6	–	15.2 ± 1.3	–	[49]
Benznidazole	–	–	–	24.2 ± 1.9 **SI:** 0.8	–	13.6 ± 0.9	[31]
dmtp	36.7 ± 2.2 **SI:** 2.7	71.7 ± 5.4 **SI:** 1.4	38.9 ± 3.1 **SI:** 2.6	48.0 ± 2.9 **SI:** 2.1	98.7 ± 9.2	101.2 ± 8.1	[34]
$AgBF_4$	> 50 **SI:** < 1	> 50 **SI:** < 1	> 50 **SI:** < 1	49.2 ± 3.9 **SI:** < 1	< 50	< 50	
$AgClO_4$	19.3 ± 1.5 **SI:** < 2.6	22.6 ± 1.8 **SI:** < 2.2	17.6 ± 1.4 **SI:** < 2.8	15.4 ± 1.2 **SI:** < 3.2	< 50	< 50	
$AgNO_3$	18.1 ± 1.4 **SI:** < 2.8	20.9 ± 1.7 **SI:** < 2.4	23.5 ± 1.9 **SI:** < 2.1	16.2 ± 1.3 **SI:** < 3.1	< 50	< 50	
1	< 1 **SI:** > 60.2	< 1 **SI:** > 60.2	< 1 **SI:** > 60.2	< 1 **SI:** > 101.5	60.2 ± 4.8	101.5 ± 8.1	
2	< 1 **SI:** > 1000	< 1 **SI:** > 1000	< 1 **SI:** > 1000	< 1 **SI:** > 293.8	> 1000	293.8 ± 23.5	
3	< 1 **SI:** > 59.1	< 1 **SI:** > 59.1	< 1 **SI:** > 59.1	< 1 **SI:** > 223.9	59.1 ± 4.7	223.9 ± 17.9	
Ni-dmtp	27.7 ± 3.8 **SI:** 32.6	45.1 ± 3.5 **SI:** 20.0	–	38.2 ± 9.0 **SI:** > 26.2	904 ± 63	> 1000	[32]
Cu-dmtp	97.7 ± 15.4 **SI:** 15.1	35.6 ± 3.7 **SI:** 54.2	–	19.2 ± 11 **SI:** 16.5	558.6 ± 9.8	420.3 ± 6.5	[32]
La-mtpO	2.8 ± 0.5 **SI:** 54.1	5.3 ± 0.1 **SI:** 28.6	–	3.7 ± 0.1 **SI:** 38.0	151.6 ± 6.4	140.8 ± 11.6	[37]
Eu-mtpO	17.7 ± 1.5 **SI:** 49.9	24.7.8 ± 2.3 **SI:** 78.8	–	15.8 ± 0.9 **SI:** 62.9	883 ± 24	995 ± 35	[37]

Ni-dmtp: $[Ni(dmtp)_2(H_2O)_4](ClO_4)_2{\cdot}2dmtp{\cdot}2H_2O$; **Cu-dmtp**: $[Cu(dmtp)_4(H_2O)_4](ClO_4)_2{\cdot}2H_2O$; **La-mtpO**: $[La(mtpO)_3(H_2O)_6]{\cdot}9H_2O$ **Eu-mtpO**: $[Eu(mtpO)_3(H_2O)_6]{\cdot}9H_2O$.
The results presented are averages of three separate determinations.
[a] The concentration required to obtain 50% inhibition, calculated through a linear regression analysis from the Kc values at the concentration employed (1, 10, 25 and 100 μM for promastigote and epimastigote forms of *Leishmania* spp. and *Trypanosoma cruzi* respectively and 50, 100, 200 and 400 μM for host cells).
[b] Selectivity index (SI) = IC_{50} against J774.2 macrophages or Vero cells/IC_{50} parasite (promastigote or epimastigote forms respectively).

indexes much lower than those of the Ag-dmtp complexes. This reassures us that the presence of both silver and dmtp is necessary for getting the best results.

Regarding the mechanism of actuation of the compounds, previous studies showed that this kind of compounds [31,33,49–51] and other similar complexes and organic ligands [52,53] can alter the metabolic route of the parasites, so we focused on this point to figure out the way the compounds were acting over the parasites. As far as it is known to the date, none of the studied parasites is able to completely metabolize glucose into CO_2 under aerobic conditions, so great part of their carbon skeletons are excreted to the medium as fermented metabolites. The nature and concentration of those depend on the considered species. [54] In case of the metabolic routes are affected, excreted metabolites and their percentual amount relative to control can be observed by ^1H NMR analysis of the culture medium. In our case, these alterations can be observed in Figs. 6 and 7, that show the percentual variations of selected excreted metabolites for *L. infantum* and *L. braziliensis* when treated with a 0,5 μM concentration of the compounds.

As it is seen in the figures, the mainly affected metabolites are D-lactate, for both species; L-alanine in the case of *L. infantum* and acetate in the case of *L. braziliensis*, which are also some of the catabolites affected by tested drugs in previous studies of metabolic divergences [31,33,49–53]. These alterations show that the compounds affect to the metabolic routes of the parasites, either inhibiting or overexpressing some enzymes responsible for the regulation of the production and excretion of these metabolites. The alteration in the major production and excretion of the mentioned catabolites suggests that the assayed compounds probably affect to the metabolic route of the parasites at the pyruvate stage of the glucose metabolism, since these metabolites are strongly related to the transformation of PEP in pyruvate by the action

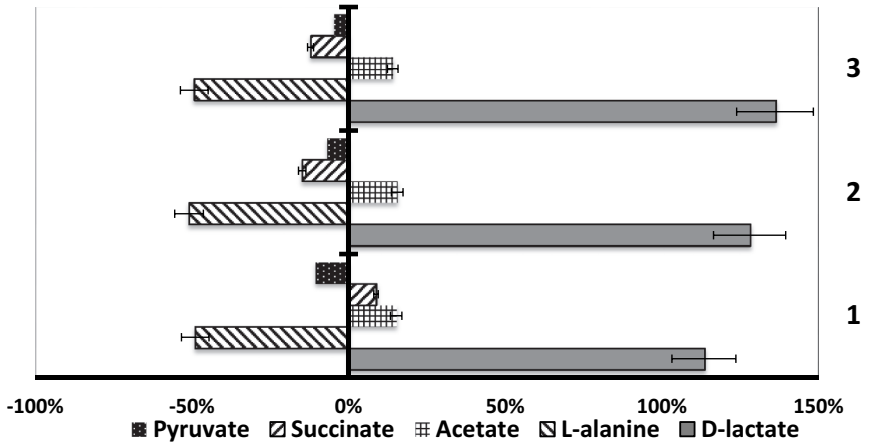

Fig. 6. Percentual variations on metabolites of *L. infantum* related to control.

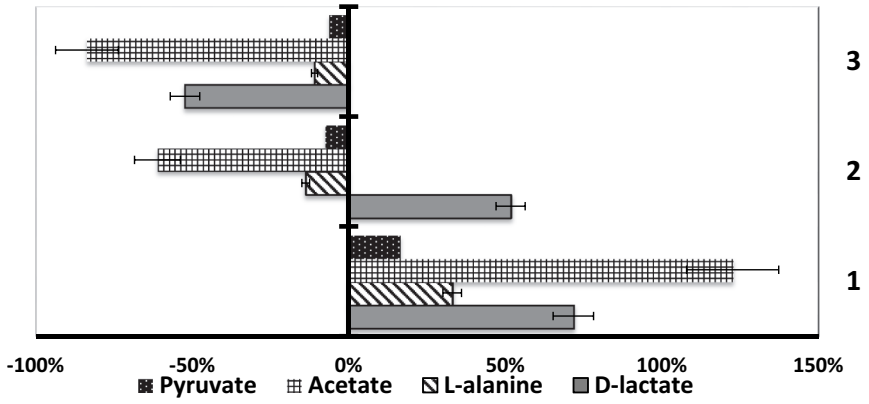

Fig. 7. Percentual variations on metabolites of *L. braziliensis* related to control.

of pyruvate kinase or pyruvate phosphatase dikinase [55]. The inhibition of the parasites growth could then be due to mentioned metabolism dysregulations provoked by the silver drugs, which can also affect to mitochondrial metabolism. However, further studies of this would be necessary to completely define the mechanism of actuation of the tested drugs.

4. Conclusions

We have synthesized two new silver complexes, which contain **dmtp**, a nucleobase analogue in neutral form. Crystallographic studies showed that both complexes are conformed by dinuclear silver entities, with two or three bridging ligands. Both compounds displayed interesting photoluminescent properties, with the main emission in the visible range, in contrast with the free ligand which emits mainly in the UV.

In vitro antiparasitic activity of these two compounds and another previously reported one has been tested against *L. infantum*, *L. donovani*, *L. braziliensis* and *T. cruzi*. Their *in vitro* activity highly exceeded that of the current reference drugs for treatment of leishmaniasis and Chagas disease. In addition, the three compounds showed much higher selectivity towards parasites when compared to host cells in culture, and especially compound **2** showed specificity more than a thousand times higher than the reference drugs. The results also improve those of previously reported complexes of triazolopyrimidine derivatives.

In sum, the work described here shows encouraging results in the development of new more specific and effective silver-based antiparasitic drugs with minimal toxicity to host cells.

Acknowledgements

This work was financially supported by the Junta de Andalucía (research groups FQM-195 and CTS944) and the Spanish Ministry of Science, Innovation and Universities (University Faculty Training Plan – FPU Grants).

Abbreviations

tp	1,2,4-triazolo[1,5-*a*]pyrimidine
dmtp	5,7-dimethyl[1,2,4]triazolo[1,5-*a*]pyrimidine
7-atp	7-amino[1,2,4]triazolo[1,5-*a*]pyrimidine
HmtpO	7-hydroxy-5-methyl[1,2,4]triazolo[1,5-*a*]pyrimidine
mtpO$^-$	5-methyl[1,2,4]triazolo[1,5-*a*]pyrimidin-7-olate
Hdmax	4,6-dimethyl-1,2,3-triazolo-[4,5-d]-pyrimidin-5,7-dione
MTL	Medium Trypanosome Liquid
HBSS	Hank's Balanced Salt Solution
MEM	Minimal Essential Medium
FBS	Fetal bovine serum
RPMI	Roswell Park Memorial Institute
SI	Selectivity index
IC	Inhibitory concentration
IC_{50}	Half maximal inhibitory concentration

Appendix A. Supplementary data

Supplementary data to this article can be found online at https://doi.org/10.1016/j.jinorgbio.2019.110810.

References

[1] J.M. Salas, M.A. Romero, M.P. Sánchez, M. Quirós, Coord. Chem. Rev. 193–195 (1999) 1119–1142.
[2] I. Łakomska, M. Fandzloch, Coord. Chem. Rev. 327–328 (2016) 221–241.
[3] J.M. Salas, A.B. Caballero, G.M. Esteban-Parra, J.M. Méndez-Arriaga, Curr. Med. Chem. 24 (2017) 2796–2806.
[4] M.A. Romero, J.M. Salas, M. Quirós, D.J. Williams, J. Molina, Trans. Met. Chem. 18 (1993) 595–598.
[5] M.A. Romero, J.M. Salas, M. Quirós, M.P. Sánchez, J. Romero, D. Martin, Inorg. Chem. 33 (1994) 5477–5481.
[6] J.M. Salas, A. Rahmani, M.A. Romero, M. Quirós, E.R. Tiekink, J. Chem. Crystallogr. 24 (1994) 669–673.
[7] J.A.R. Navarro, M.A. Romero, J.M. Salas, M. Quirós, J.E. Bahraoui, J. Molina, Inorg. Chem. 35 (1996) 7829–7835.
[8] M.A. Haj, M. Quirós, J.M. Salas, Dalton Trans. 24 (2002) 4740–4745.
[9] M.A. Haj, M. Quirós, J.M. Salas, J.A. Dobado, J. Molina, M.G. Basallote, M.A. Manez, Eur. J. Inorg. Chem. 4 (2002) 811–818.
[10] C.R. Maldonado, M. Quirós, J.M. Salas, Polyhedron 27 (2008) 2779–2784.
[11] A.B. Caballero, A. Rodríguez-Diéguez, L. Lezama, E. Barea, J.M. Salas, Dalton Trans. 40 (2011) 5180–5187.
[12] A.B. Caballero, A. Rodríguez-Diéguez, L. Lezama, J.M. Salas, Cryst. Growth Des. 12 (2012) 3583–3593.
[13] J.M. Méndez-Arriaga, G.M. Esteban-Parra, M.J. Juarez, A. Rodríguez-Diéguez, M. Sánchez-Moreno, J. Isac-Garcia, J.M. Salas, J. Inorg. Biochem. 175 (2017) 217–224.
[14] E. Szłyk, L. Pazderski, I. Łakomska, L. Kozerski, J. Sitkowski, Mag. Res. Chem. 40 (2002) 529–532.
[15] M.A. Girasolo, D. Schillaci, C. Salvo, G. Barone, A. Silvestri, G. Ruisi, J. Organomet. Chem. 691 (2006) 693–701.
[16] J. Ruiz, M. Dolores Villa, N. Cutillas, G. López, C. de Haro, D. Bautista, V. Moreno, L. Valencia, Inorg. Chem. 47 (2008) 4490–4505.
[17] J. Huub Adriaanse, S.H.C. Askes, Y. van Bree, S. van Oudheusden, E.D. van den Bos, E. Guenay, I. Mutikainen, U. Turpeinen, G.A. van Albada, J.G. Haasnoot, Polyhedron 28 (2009) 3143–3149.
[18] J.M. Balkaran, S.C.P. van Bezouw, J. van Bruchem, J. Verasdonck, P.C. Verkerk, A.G. Volbeda, I. Mutikainen, U. Turpeinen, G.A. van Albada, P. Gamez, J.G. Haasnoot, J. Reedijk, Inorg. Chim. Acta 362 (2009) 861–868.
[19] M. Fandzloch, A. Wojtczak, J. Sitkowski, I. Łakomska, Polyhedron 67 (2014) 410–415.
[20] L. Lu, B. Mu, N. Li, R. Huang, Chem. Res. Chin. U. 31 (2015) 712–718.
[21] I. Łakomska, H. Kooijman, A.L. Spek, W. Shen, J. Reedijk, Dalton Trans. 48 (2009) 10736–10741.
[22] M.A. Girasolo, A. Attanzio, P. Sabatino, L. Tesoriere, S. Rubino, G. Stocco, Inorg. Chim. Acta 423 (2014) 168–176.
[23] M.A. Girasolo, C. Di Salvo, D. Schillaci, G. Barone, A. Silvestri, G. Ruisi, J. Organomet. Chem. 690 (2005) 4773–4783.
[24] G. Ruisi, L. Canfora, G. Bruno, A. Rotondo, T.F. Mastropietro, E.A. Debbia, M.A. Girasolo, B. Megna, J. Organomet. Chem. 695 (2010) 546–551.
[25] WHO, Control of the Leishmaniasis: Report of a Meeting of the WHO Expert Committee on the Control of Leishmaniasis, Geneva, 22–26 March 2010, W.H.O. Tech. Rep. Ser 949 (2010), pp. 91–107.
[26] P.J. Hotez, D.H. Molyneux, A. Fenwick, J. Kumaresan, S.E. Sachs, J.D. Sachs, L. Savioli, N. Engl. J. Med. 357 (2007) 1018–1027.
[27] D. Gambino, L. Otero, Inorg. Chim. Acta 393 (2012) 103–114.
[28] B. Demoro, C. Sarniguet, R. Sánchez-Delgado, M. Rossi, D. Liebowitz, F. Caruso, C. Olea-Azar, V. Moreno, A. Medeiros, M.A. Comini, L. Otero, D. Gambino, Dalton Trans. 41 (2012) 1534–1543.
[29] M.I.F. Barbosa, R.S. Correa, K.M. de Oliveira, C. Rodrigues, J. Ellena, O.R. Nascimento, V.P.C. Rocha, F.R. Nonatoc, T.S. Macedoc, J. Inorg. Biochem. 136 (2014) 33–39.
[30] E. Rodríguez-Arce, I. Machado, B. Rodríguez, M. Lapier, M.C. Zúñiga, J.D. Maya, C. Olea-Azar, L. Otero, D. Gambino, J. Inorg. Biochem. 170 (2017) 125–133.
[31] A.B. Caballero, C. Marín, A. Rodríguez-Diéguez, I. Ramírez-Macías, E. Barea, M. Sánchez-Moreno, J.M. Salas, J. Inorg. Biochem. 105 (2011) 770–776.
[32] A.B. Caballero, A. Rodríguez-Diéguez, M. Quirós, J.M. Salas, Ó. Huertas, I. Ramírez-Macías, F. Olmo, C. Martin, G. Chaves-Lemaur, R. Gutierrez-Sánchez, M. Sánchez-Moreno, Eur. J. Med. Chem. 85 (2014) 526–534.
[33] S. Boutaleb-Charki, C. Marín, C.R. Maldonado, M.J. Rosales, J. Urbano, R. Gutierrez-Sánchez, M. Quirós, J.M. Salas, M. Sánchez-Moreno, Drug. Metab. Lett. 3 (2009) 35–44.
[34] A.B. Caballero, C. Marín, I. Ramírez-Macías, A. Rodríguez-Diéguez, M. Quirós, J.M. Salas, M. Sánchez-Moreno, Polyhedron 33 (2012) 137–144.
[35] J.M. Méndez-Arriaga, I. Oyarzabal, G. Escolano, A. Rodríguez-Diéguez, M. Sánchez-Moreno, J.M. Salas, J. Inorg. Biochem. 180 (2018) 26–32.
[36] M. Fandzloch, J.M. Méndez-Arriaga, M. Sánchez-Moreno, A. Wojtczak, J. Jezierska, J. Sitkowski, J. Wisniewska, J.M. Salas, I. Lakomska, J. Inorg. Biochem. 176 (2017) 144–155.
[37] A.B. Caballero, A. Rodríguez-Diéguez, J.M. Salas, M. Sánchez-Moreno, C. Marin, I. Ramírez-Macías, N. Santamaria-Diaz, R. Gutiérrez-Sánchez, J. Inorg. Biochem. 138 (2014) 39–46.
[38] M.A. Romero, J.M. Salas, M. Quirós, M.P. Sánchez, J. Molina, J. El Bahraoui, R. Faure, J. Mol. Struct. 354 (1995) 189–195.
[39] Bruker Apex2, Bruker AXS Inc., 2004, Madison, Wisconsin, USA.
[40] G.M. Sheldrick, SADABS, Program for Empirical Adsorption Correction, Institute for Inorganic Chemistry, University of Gottingen, Germany, 1996.
[41] G.M. Sheldrick, Acta Cryst. C 71 (2015) 3–8.
[42] P. González, C. Marín, I. Rodríguez-González, A.B. Hitos, M.J. Rosales, M. Reina, J.G. Díaz, A. González-Coloma, M. Sánchez-Moreno, Int. J. Antimicrob. Agents 25 (2005) 136–141.
[43] C. Fernández-Becerra, M. Sánchez-Moreno, A. Osuna, F.R. Opperdoes, J. Euk. Microbiol. 44 (1997) 523–529.
[44] M. Abul Haj, M. Quirós, J.M. Salas, R. Faure, J. Chem. Soc. Dalton Trans. (2001) 1798–1801.
[45] J.A.R. Navarro, J.M. Salas, M.A. Romero, R. Faure, J. Chem. Soc. Dalton Trans. (1998) 901–904.
[46] A.B. Caballero, A. Rodríguez-Diéguez, E. Barea, M. Quirós, J.M. Salas, Cryst. Eng. Comm. 12 (2010) 3038–3045.
[47] L. Lü, B. Mu, N. Li, R. Huang, Chem. Res. Chin. Univ. 31 (2015) 712–718.
[48] A.B. Caballero, A. Rodríguez-Diéguez, M. Quirós, L. Lezama, J.M. Salas, Inorg. Chim. Acta 37 (2011) 194–201.
[49] I. Ramírez-Macías, C. Marin, J.M. Salas, A. Caballero, M.J. Rosales, N. Villegas, A. Rodríguez-Diéguez, E. Barea, M. Sánchez-Moreno, J. Antimicrob. Chemother. 66 (2011) 813–819.
[50] C.R. Maldonado, C. Marín, F. Olmo, O. Huertas, M. Quirós, M. Sánchez-Moreno, M.J. Rosales, J.M. Salas, J. Med. Chem. 53 (2010) 6964–6972.
[51] I. Ramírez-Macías, C.R. Maldonado, C. Marín, F. Olmo, R. Gutiérrez-Sánchez, M.J. Rosales, M. Quirós, J.M. Salas, M. Sánchez-Moreno, J. Inorg. Biochem. 112 (2012) 1–9.
[52] Á. Martín-Montes, R. Ballesteros-Garrido, R. Martín-Escolano, C. Marín, R. Guitiérrez-Sánchez, B. Abarca, R. Ballesteros, M. Sánchez-Moreno, RSC Adv. 7 (2017) 15715–15726.
[53] K. Urbanová, I. Ramírez-Macías, R. Martín-Escolano, M.J. Rosales, O. Cussó, J. Serrano, A. Company, M. Sánchez-Moreno, M. Costa, X. Ribas, C. Marín, Molecules 24 (2019) 134, https://doi.org/10.3390/molecules24010134.
[54] F. Bringaud, L. Rivière, V. Coustou, Mol. Biochemm Parasitol. 149 (2006) 1–9.
[55] P.A.M. Michels, F. Bringaud, M. Herman, V. Hannaert, Biochim. Biophys. Acta 1763 (2006) 1463–1477.